



ELSEVIER

Contents lists available at SciVerse ScienceDirect

Talanta

journal homepage: [www.elsevier.com/locate/talanta](http://www.elsevier.com/locate/talanta)

# Flow electrochemical analyses of zinc by stripping voltammetry on graphite felt electrode

B. Feier<sup>a,b</sup>, D. Floner<sup>a</sup>, C. Cristea<sup>b</sup>, E. Bodoki<sup>b</sup>, R. Sandulescu<sup>b</sup>, F. Geneste<sup>a,\*</sup>

<sup>a</sup> Université de Rennes 1, UMR-CNRS 6226, Institut des Sciences Chimiques de Rennes, Equipe MaCSE, Campus de Beaulieu, 35042 Rennes cedex, France

<sup>b</sup> Iuliu Hatieganu University of Medicine and Pharmacy, Faculty of Pharmacy, 4 Pasteur str, 400012 Cluj-Napoca, Romania

## ARTICLE INFO

### Article history:

Received 30 March 2012

Received in revised form

20 June 2012

Accepted 25 June 2012

Available online 28 June 2012

### Keywords:

Anodic stripping voltammetry

Flow analysis

Graphite felt

Zinc

Trace analysis

Porous electrode

## ABSTRACT

A flow sensor for trace analysis of zinc, using graphite felt as working electrode is reported here. A flow cell, well-adapted to 3-D porous electrodes and capable to do both the preconcentration step at a cathodic potential and the stripping of the zinc was successfully developed. It was demonstrated that this cell allows to obtain better electrochemical signals for  $Zn^{2+}$  compared to a standard three-electrodes cell and that the percolation during accumulation increases the kinetics of electrodeposition. The influence on  $Zn^{2+}$  signal of the deposition potential, the time of deposition and the flow rate was studied. The resulting sensor shows a linear response towards  $Zn^{2+}$  with a linear range of  $10^{-6}$ – $10^{-4}$  M and a limit of detection of  $5 \times 10^{-7}$  M for an analysis time of 5 min. The interferences study showed that the  $Cr^{3+}$ ,  $Pb^{2+}$ ,  $Cd^{2+}$  ions have a small effect on the Zn electrochemical signal, whereas  $Fe^{3+}$ ,  $Cu^{2+}$ ,  $Co^{2+}$  and  $Ni^{2+}$  ions strongly influence it. The electrode was tested on real samples (tap water spiked with  $Zn^{2+}$ , food supplement) with a good recovery by applying the standard addition method.

© 2012 Elsevier B.V. All rights reserved.

## 1. Introduction

Continuous flow analytical systems are advantageous because they are easily automatable and they approach the ideal real-time analysis. Electrochemical flow detection has been the subject of investigations in many areas such as environment, agriculture, food control and health as independent analytical systems or combined with chromatography or capillary electromigration methods [1–5]. Stripping voltammetry is one of the most sensitive analytical methods for trace analysis. Flow systems are particularly advantageous in stripping voltammetry analysis since they enhance mass transport and so increase the efficiency of the preconcentration step [1]. Some studies have dealt with static mercury drop [6–8] but more attention has been given on solid electrodes that are better adapted to flow systems. Stripping voltammetry analyses in flow systems have been performed on working electrodes of different nature, such as carbon [9], gold [10], mercury with Hg films [11–14] or bismuth [15–17]. These last ones have the advantage to exhibit a large potential window. The geometry of the electrode plays also a role in the improvement of the flow analytical system. Porous working electrodes have been used for their high surface area and good hydrodynamic properties, resulting in a high coulometric efficiency and low detection limits. Porous electrodes of different nature exist, such as nickel [18], copper [19] and

bismuth [20]. However, to our knowledge, only porous carbon electrodes have been studied for stripping voltammetry analysis in flow. Thus, reticulated vitreous carbon (RVC) possess high void volume (90–97% depending on the standard porosity grade) leading to low resistance to fluid flow, good electrical conductivity and high surface area ( $65 \text{ cm}^2 \text{ cm}^{-3}$ ) [21–26].

Graphite felts are formed of graphite fibers of around  $10 \mu\text{m}$  of diameter. Due to their high specific surface area (from  $1$  to  $1200 \text{ m}^2 \text{ g}^{-1}$ ), they have been used in electrosynthesis [27–31]. Recently, we have also reported the interest of graphite felt electrodes for application in flow electroanalysis [32–34]. Interestingly, this material has a high surface area ( $616 \text{ cm}^2 \text{ cm}^{-3}$ ), a good conductivity and presents good hydrodynamic properties due to its high void volume (around 90%).

Stripping voltammetry analysis on graphite felt with preconcentration of heavy metals by electrodeposition performed by flowing the solution through the porous electrode is described. Zinc has been chosen as analyte since its determination in environmental and biological samples is important. Indeed, zinc is an essential trace element for growth and development and its deficit can affect multiple organs [35,36]. As expected, we showed that passing the solution through the electrode increased the kinetics of electrodeposition, compared with static systems. A flow electrochemical cell well-adapted to 3-D porous electrodes, which enhances the electrochemical response is also presented. The analytical conditions were optimized, leading to the detection of zinc with good sensitivities.

\* Corresponding author. Tel.: +33 2 23 23 59 65; fax: +33 2 23 23 59 67.  
E-mail address: [florence.geneste@univ-rennes1.fr](mailto:florence.geneste@univ-rennes1.fr) (F. Geneste).

## 2. Experimental part

### 2.1. Reagents and materials

The graphite felt (RVG 4000) and the papyex were obtained from Mersen (France). The specific area of the felt measured by the BET method is  $0.7 \text{ m}^2 \text{ g}^{-1}$  and its density is  $0.088 \text{ g cm}^{-3}$ . The diameter of a fiber is around  $20 \mu\text{m}$ . Iron(III) nitrate nonahydrate, Chromium(III) nitrate monohydrate, Lead(II) nitrate, copper(II) tetrafluoroborate monohydrate, zinc(II) nitrate hexahydrate, cobalt(II) nitrate hexahydrate and sodium tetrafluoroborate were purchased from Acros and nickel(II) nitrate hexahydrate, cadmium(II) nitrate tetrahydrate from Aldrich. All solutions were prepared with ultrapure water ( $18.2 \text{ M}\Omega$ , Millipore Simplicity). All glassware and flow reactor were rinsed with a 10%  $\text{HNO}_3$  solution followed by ultrapure water before use to avoid metal contamination.

### 2.2. Electrochemical measurement

Voltammetric experiments were carried out using a Versa-STAT3 AMETEK Model (Princeton Applied Research) potentiostat/galvanostat. For electrochemical analyses performed in a standard three-electrodes configuration, a graphite felt working electrode (cylinder of diameter 1 cm and thickness 6 mm) fixed to a platinum wire, a platinum wire auxiliary electrode, and a saturated calomel reference electrode (SCE) were used. The electrochemical flow analyses in flow were carried out in a flow electrochemical cell (Fig. 1).

The main body of the cell was made of Teflon. The graphite felt (cylinder of diameter 1 cm and thickness 6 mm) was positioned between two counter electrodes (papyex). Linear sweep stripping voltammetry analyses were performed in ultrapure water, containing  $0.1 \text{ M NaBF}_4$ , at a  $100 \text{ mV s}^{-1}$  scan rate, under a dinitrogen atmosphere.

### 2.3. General procedure

Aqueous solutions containing the analyte were deaerated with nitrogen and passed through the flow electrochemical cell using a peristaltic pump (Minipuls 3, Gilson) at continuous flow rate (studied range:  $0.8\text{--}4 \text{ mL min}^{-1}$ ). The accumulation step was performed by applying a potential of  $-1.4 \text{ V}_{\text{SCE}}$  (studied range:  $-1.9$  to  $-1.2 \text{ V}_{\text{SCE}}$ ) for an accumulation time of 4 min (studied range 1–20 min). Subsequently, the pump was stopped and after an equilibration time of 1 min, a linear anodic scan was carried out from the deposition

potential  $-1.4$  to  $0.5 \text{ V}_{\text{SCE}}$  at a scan rate of  $100 \text{ mV s}^{-1}$ , while the anodic signal is obtained. These conditions (potential up to  $0.5 \text{ V}_{\text{SCE}}$ ) were necessary for desorption of zinc from the electrode surface. The electrode was then rinsed in flow.

### 2.4. Real samples analysis

A solution of  $2.5 \times 10^{-5} \text{ M}$  of zinc in tap water was prepared by dilution of a  $10^{-2} \text{ M}$  stock solution, adding at the end  $\text{NaBF}_4$  to obtain  $0.1 \text{ M}$  concentration of the supporting electrolyte. Three other solutions of  $2 \times 10^{-5}$ ,  $1.5 \times 10^{-5}$  and  $10^{-5} \text{ M}$  of zinc in tap water were prepared by successive dilutions of the  $2.5 \times 10^{-5} \text{ M}$  zinc solution with  $0.1 \text{ M NaBF}_4$  in tap water. They were analyzed by the procedure described above, giving rise to a mean of the electrochemical signal due to the presence of zinc in tap water. The concentration of zinc was then determined by the standard addition method ( $n=3$ ).

The same procedure was applied to an oral solution containing zinc (Oligosol from Labcatal). Using the declared concentration in zinc ( $67.4 \mu\text{g Zn}^{2+}/2 \text{ ml}$  oral solution), four solutions of  $2 \times 10^{-6}$ ,  $3 \times 10^{-6}$ ,  $4 \times 10^{-6}$  and  $5 \times 10^{-6} \text{ M}$  of zinc in ultrapure water and  $0.1 \text{ M NaBF}_4$  were prepared by diluting the Oligosol solution. The concentration of zinc was then determined by the standard addition method ( $n=3$ ).

## 3. Results and discussion

### 3.1. Analysis

Experiments were performed with a graphite felt electrode (cylinder of diameter 1 cm and thickness 6 mm) in a cell adapted for flow electroanalysis with 3D porous electrodes (Fig. 1). The graphite felt was located in the middle of two counter-electrodes to improve the homogeneity of the potential distribution in the three dimensional working electrode [37].

The reference electrode was positioned in the middle of the felt. The analyses were carried out by linear sweep stripping voltammetry (LSSV) in a  $0.1 \text{ M}$  aqueous solution of  $\text{NaBF}_4$ . The preconcentration step was performed by reducing the  $\text{Zn}^{2+}$  ions at  $-1.4 \text{ V}_{\text{SCE}}$  for 5 min and then the potential was varied from  $-1.4$  to  $0.5 \text{ V}_{\text{SCE}}$ . With the electrochemical flow cell, the deposition step was performed either in a static mode for 5 min or by flowing the solution through the porous electrode for 4 min with subsequent 1 min in static mode (Fig. 2).

One minute in static mode was necessary to decrease the initial current intensity before the potential was swept in the anodic direction and to obtain a well-defined stripping peak of Zn. Lower values gave rise to less reproducibility due to difficult peak integration. The same experiment was carried out with a graphite felt of same dimensions used as working electrode in a standard three-electrode cell without stirring for comparison with the results obtained with the flow cell in static mode. The electrochemical flow cell appropriate for 3D electrodes [37] led to the improvement of the electrochemical response compared with the standard three-electrodes cell; with the flow cell, even in static mode, the initial current intensity at  $-1.4 \text{ V}_{\text{SCE}}$  was less negative and a higher stripping peak of Zn was obtained. Furthermore, the signal was significantly higher when the solution passed through the porous electrode during the electrodeposition step. This result emphasized the interest of the preconcentration in flow, compared with a static system, to increase the kinetics of electrodeposition and to reduce the analysis time.

Several parameters were optimized to enhance the zinc signal.  $\text{Zn}^{2+}$  ions were deposited at different potentials ranging from  $-1.2$  to  $-1.9 \text{ V}_{\text{SCE}}$ . The stripping peak was visible for potentials higher than  $-1.2 \text{ V}_{\text{SCE}}$  and reached a maximum for electrodeposition performed at  $-1.7 \text{ V}_{\text{SCE}}$  (Fig. 3).

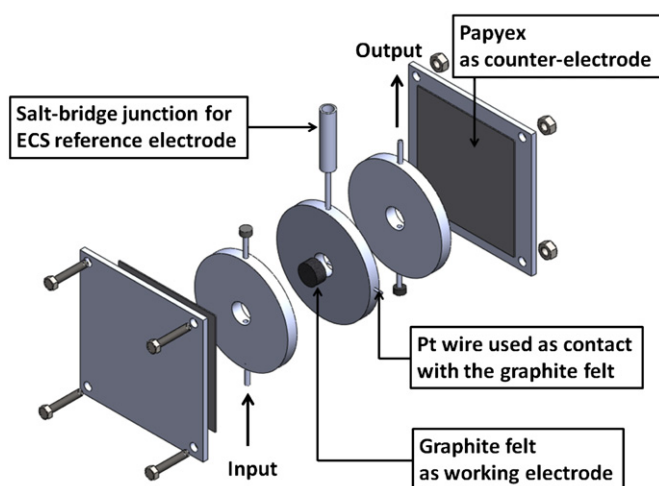
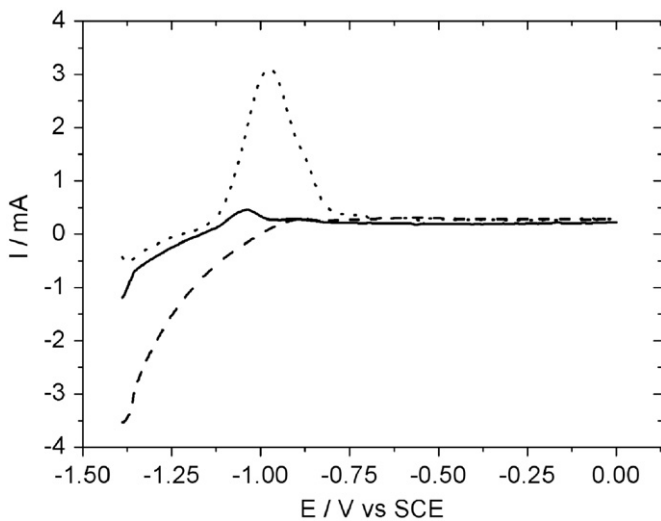


Fig. 1. Solidworks image of the electrochemical flow cell.

The peak started to broaden at more cathodic potentials than  $-1.5 V_{SCE}$  to be finally divided into two distinct peaks. Peak splitting has already been observed in anodic stripping voltammetry and is linked to the electrodeposition potential and to the analyte concentration [38–40]. The reasons seem to be related to the accumulation of the reduced metal on the electrode surface in different ways, in an external or a deep layer. A reduction potential of  $-1.4 V_{SCE}$  was kept in the following experiments in order to obtain a well-defined Zn peak and facilitate its integration.

Different times for the reduction step were also tested (Fig. 4).

The zinc electrochemical response increased linearly with the deposition time, meaning that improved sensitivities can be achieved with longer analysis time. A deposition time of 5 min including 1 min of static mode was then used to avoid too long analysis time.



**Fig. 2.** LSSVs of  $10^{-5}$  M zinc solution on a graphite felt electrode (cylinder of diameter 1 cm and thickness 6 mm) in a 0.1 M aqueous solution of  $NaBF_4$  with reduction at  $-1.4 V_{SCE}$  for 5 min in static mode (—) and 4 min in flow ( $0.8 \text{ mL min}^{-1}$ ) and 1 min in static mode (...). The same experiment was performed in a standard three-electrodes cell for comparison (---), Scan rate:  $0.1 \text{ V s}^{-1}$ .

To appreciate the effect of the flow rate on the electrochemical signal of zinc, the graphite felt was percolated with a  $10^{-5}$  M zinc solution, using flow rates ranging from  $0.8$  to  $4 \text{ mL min}^{-1}$ . The experiment was performed with deposition potentials of  $-1.5$  and  $-1.4 V_{SCE}$  for 5 min. The electrical charge of zinc measured after LSSV analysis increased with the flow rate to reach a plateau for flow rate higher than  $2\text{--}2.5 \text{ mL min}^{-1}$  (Fig. 5).

The increase of the electrochemical signal with the flow rate was expected since higher flow rate enhanced mass-transport and larger amounts of the analyte reached the electrode surface in a given time. The decrease of the slope of the curve after  $2\text{--}2.5 \text{ mL min}^{-1}$  is unclear. However, this phenomenon has already been observed and attributed to a lower adhesion of the metal film to the surface of the electrode or to the high convection, preventing the adsorption/desorption equilibrium under natural conditions to occur during the accumulation step [41–43].

Repeated analyses of a  $10^{-5}$  M zinc solution were performed in the conditions we retained to draw the calibration curve (see

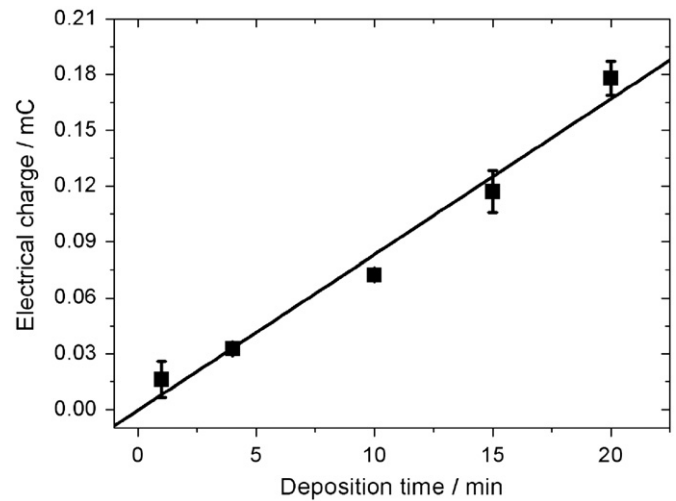


**Fig. 4.** Electrical charge calculated from LSSV analysis of zinc, upon varying the deposition time in flow. The preconcentration step was performed at  $-1.4 V_{SCE}$  using a  $10^{-6}$  M zinc solution and 0.1 M  $NaBF_4$ , in flow at  $0.8 \text{ mL min}^{-1}$  and 1 min in static mode. Error bars are based on two sample measurements.

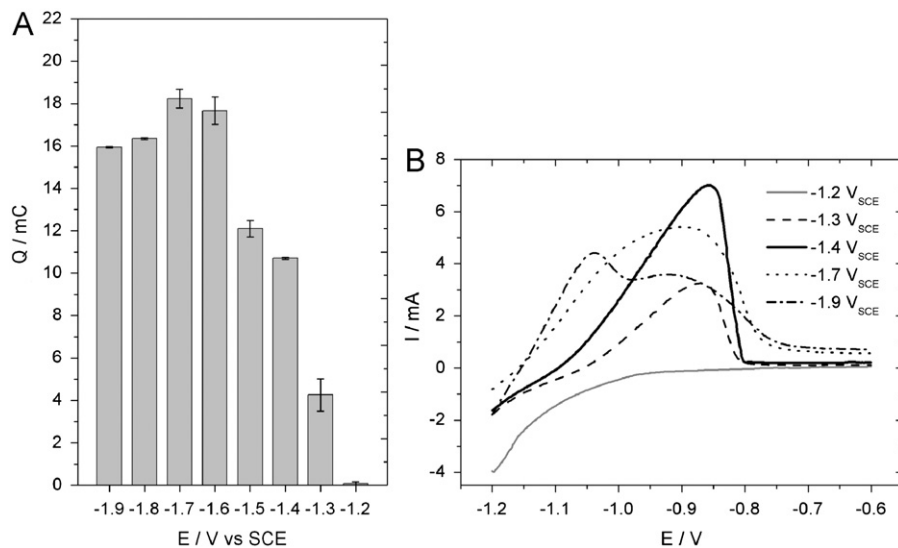


**Fig. 3.** Electrical charge (A) and LSSVs of zinc (B), as a function of reduction potential. Scan rate:  $0.1 \text{ V s}^{-1}$ . The preconcentration step was performed using a  $10^{-5}$  M zinc solution and 0.1 M  $NaBF_4$ , in flow at  $2 \text{ mL min}^{-1}$  for 4 min and 1 min of equilibrium. Error bars are based on two sample measurements.

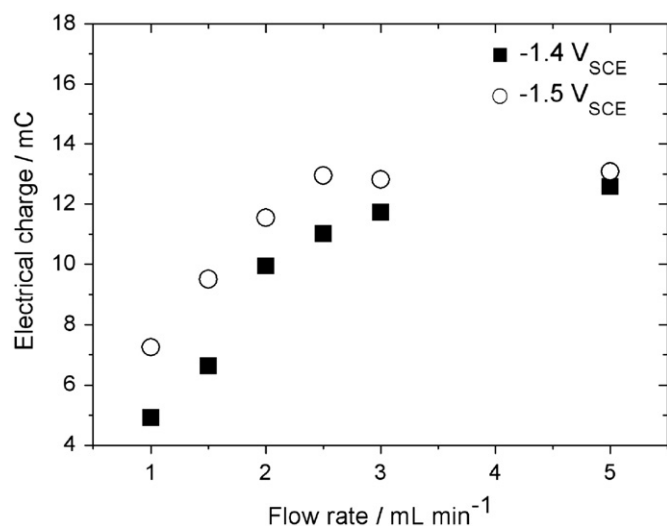


**Fig. 5.** Electrical charge calculated from LSSV analysis of zinc, upon varying the flow rate. The preconcentration step was performed at  $-1.4$  and  $-1.5$  V<sub>SCE</sub> using a  $10^{-5}$  M zinc solution and  $0.1$  M NaBF<sub>4</sub>, in flow for 4 min and 1 min in static mode.

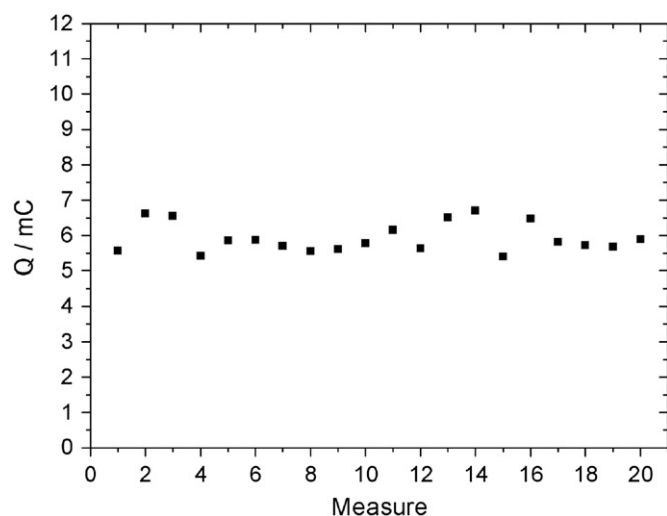


**Fig. 6.** Successive analyses of zinc. The preconcentration step was performed at  $-1.4$  V<sub>SCE</sub> with a  $10^{-5}$  M zinc solution and  $0.1$  M NaBF<sub>4</sub>, in flow at  $0.8$  mL min<sup>-1</sup> for 4 min and 1 min in static mode.

below). As seen in Fig. 6, the electrochemical signal was stable with a standard deviation of  $0.42$  mC for 20 analyses.

### 3.2. Calibration curve and detection limit

The dependence of the electrical charge of zinc on the concentration of the analyzed solution is given in Fig. 7.

In order to use low volumes of solution, a flow rate of  $0.8$  mL min<sup>-1</sup> was used to establish the calibration curve. For decreasing the limit of detection, a higher preconcentration time and a higher flow rate should be used. The curve is linear in the range of  $10^{-6}$ – $10^{-4}$  mol L<sup>-1</sup> with a correlation coefficient of  $0.9987$ .

The limit of detection ( $3 \times$  the standard deviation of five blank determinations) was determined from Eq. 1

$$St - Sb \geq 3\sigma \quad (1)$$

where  $St$  is the gross analyte signal,  $Sb$  the field blank and  $\sigma$  the standard deviation in the field blank.

$St$  and  $Sb$  were the maximum current intensity of the Zn peak. We found a limit of detection of  $5 \times 10^{-7}$  mol L<sup>-1</sup> (32.7 ppb). This

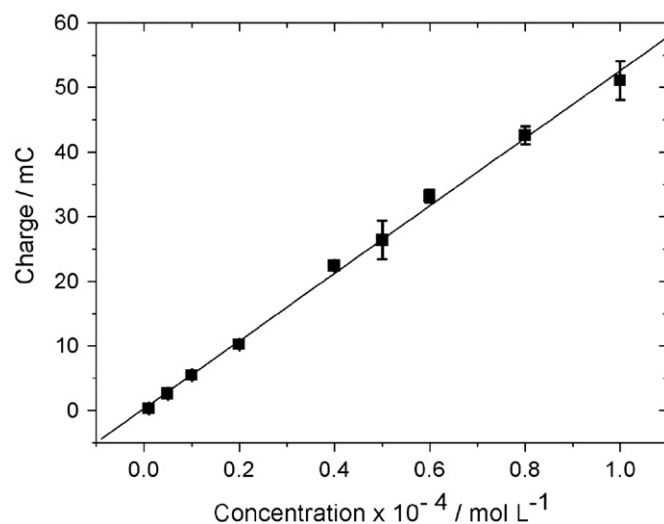


**Fig. 7.** Calibration curve of electrical charge determined by LSSV analysis at a graphite felt electrode as a function of Zn<sup>2+</sup> concentration. Error bars are based on three sample measurements.

value is a little bit higher than these previously reported in literature ( $0.4$ – $25$  ppb) [9,11,12,15]. However, it is much lower than the French drinking water guidelines for zinc set at  $7.6 \times 10^{-5}$  mol L<sup>-1</sup> (5 ppm), underlying the interest of the method that use a commercially available electrode.

### 3.3. Interference studies

The electrochemical signal of Zn<sup>2+</sup> was investigated in the presence of some common metal ion interferents Pb<sup>2+</sup>, Cd<sup>2+</sup>, Cr<sup>3+</sup>, Cu<sup>2+</sup>, Co<sup>2+</sup>, Ni<sup>2+</sup> and Fe<sup>3+</sup>. LSSV analyses were performed with a solution of Zn<sup>2+</sup> ( $10^{-5}$  mol L<sup>-1</sup>) and interferent ion. The preconcentration step was carried out at  $-1.4$  V<sub>SCE</sub> for 4 min in flow at  $1$  mL min<sup>-1</sup> and for 1 min in static mode. Interferences were observed depending on the concentration ratios of the ions. Two mechanisms can be responsible of these interferences: (i) the competition with Zn during the deposition step or (ii) the formation of an intermetallic complex with Zn [9,23]. Maximum concentrations that do not affect the zinc signal for a Zn solution of  $10^{-5}$  mol L<sup>-1</sup> are given in Table 1. Whereas in presence of Cu<sup>2+</sup>, Co<sup>2+</sup>, Ni<sup>2+</sup> and Fe<sup>3+</sup> in the same concentration, the Zn signal disappeared, Pb<sup>2+</sup>, Cr<sup>3+</sup> and Cd<sup>2+</sup> ions interfered at higher concentrations and the Zn signal was still present (75% and 20% for Cr<sup>3+</sup> and Cd<sup>2+</sup>, respectively) when a 10-fold excess of Cr<sup>3+</sup> and Cd<sup>2+</sup> was used. Thus, the concentration of metallic cations for which the zinc signal was not affected are much higher for Pb<sup>2+</sup>, Cr<sup>3+</sup> and Cd<sup>2+</sup> ions than for Cu<sup>2+</sup>, Co<sup>2+</sup>, Ni<sup>2+</sup> and Fe<sup>3+</sup>. A 100-fold excess of zinc was necessary to avoid interference with these species (Table 1). It is interesting to note that well defined stripping peaks were observed for Cd<sup>2+</sup>, Pb<sup>2+</sup> and Cu<sup>2+</sup>, at  $-0.6$ ,  $-0.3$  and  $0.4$  V<sub>SCE</sub>, respectively, showing that simultaneous detections of Zn<sup>2+</sup>, Cd<sup>2+</sup>, Pb<sup>2+</sup> and Cu<sup>2+</sup> would be possible within certain ranges of concentrations.

### 3.4. Determination of Zn<sup>2+</sup> in real samples

In order to evaluate the performance of the analytical system by practical analytical applications, the determination of Zn<sup>2+</sup> was carried out in tap water spiked with the analyte and in a food supplement without any pre-treatment (Table 2). The Zn<sup>2+</sup> concentration was determined by the standard addition method to compensate the matrix effect from real sample (Fig. 8). Good correlations between amounts determined and initial sample were obtained (recovery values of  $104 \pm 4\%$  for spiked tap water

**Table 1**  
Maximum concentrations of metallic cations that do not affect the zinc signal of a  $10^{-5}$  M Zn solution.

Interferent ion	Pb <sup>2+</sup>	Cd <sup>2+</sup>	Cr <sup>3+</sup>	Cu <sup>2+</sup>	Co <sup>2+</sup>	Ni <sup>2+</sup>	Fe <sup>3+</sup>
Concentration limit (mol L <sup>-1</sup> )	$10^{-5}$	$5 \times 10^{-6}$	$10^{-5}$	$5 \times 10^{-7}$	$10^{-7}$	$10^{-7}$	$5 \times 10^{-7}$

**Table 2**  
Determination of Zn<sup>2+</sup> with the flow electrochemical cell in real samples.

Sample	Real concentration (μmol L <sup>-1</sup> )	Measured concentration <sup>a</sup> (μmol L <sup>-1</sup> )	Recovery (%)	RSD (n=3)
Spiked tap water	5.00	5.18	104	4
Food supplement	1.031	1.053	102	3

<sup>a</sup> LSSV analysis with a preconcentration at  $-1.4$  V<sub>SCE</sub> for 4 min in flow (0.8 mL min<sup>-1</sup>) and for 1 min in static mode.

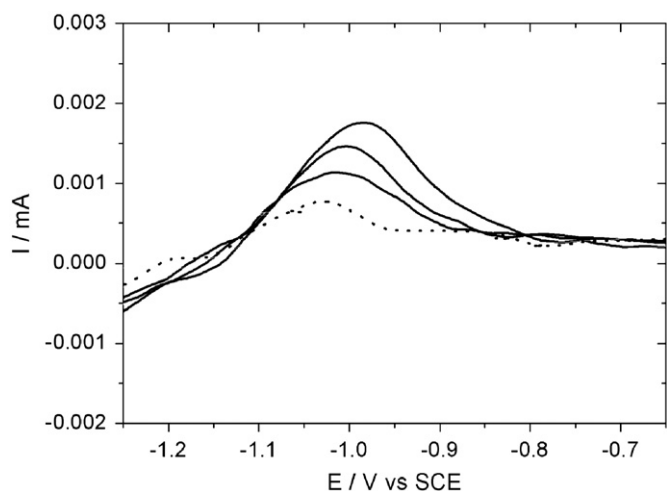


**Fig. 8.** LSSVs of Oligosol solution (···) and standard additions (—) on a graphite felt electrode (cylinder of diameter 1 cm and thickness 6 mm) in a 0.1 M aqueous solution of NaBF<sub>4</sub> with reduction at  $-1.4$  V<sub>SCE</sub> for 5 min in flow (0.8 mL min<sup>-1</sup>) and 1 min in static mode (···). Scan rate: 0.1 V s<sup>-1</sup>.

and  $102 \pm 3\%$  for food supplement), suggesting that the analytical method can be used for the analysis of Zn<sup>2+</sup> in real samples.

#### 4. Conclusion

In conclusion, it was underlined the interest of the flow analytical system for the analysis of traces, as exemplified here with zinc. The flowing process allows the enhancement of mass-transport, leading to higher electrochemical response. The LSSV analysis and the preconcentration step were performed in an electrochemical flow cell well-adapted to 3D electrodes. The performances of the flow sensor were promising since a good detection limit was obtained for zinc, using a low flow rate. The analysis of real samples led to good recovery values. The analytical system has a great potential to be used in the development of flow continuous analyzers for monitoring heavy metal ions in water samples.

#### Acknowledgments

We are grateful for the financial support to “Iuliu Hatieganu” University of Medicine and Pharmacy (project POS-DRU 88/1.5/S/56949) and to Agence Universitaire de la Francophonie (project CE/MC/288/10). We gratefully acknowledge Dominique Paris for the fabrication of the electrochemical flow cell and for the Solidworks image.

#### References

- [1] A. Economou, Anal. Chim. Acta 683 (2010) 38–51.
- [2] E.J. Llorent-Martinez, P. Ortega-Barrales, M.L. Fernandez-de Cordova, A. Ruiz-Medina, Anal. Chim. Acta 684 (2011) 30–39.
- [3] M. Trojanowicz, Anal. Chim. Acta 688 (2009) 8–35.
- [4] M. Trojanowicz, Anal. Chim. Acta 653 (2009) 36–58.
- [5] M. Trojanowicz, M. Szweczyńska, M. Wcisłoa, Electroanalysis 15 (2003) 347–365.
- [6] G. Abate, J. Lichtig, J.C. Masini, Talanta 58 (2002) 433–443.
- [7] C. Fernandez-Bobes, M.T. Fernandez-Abedul, A. Costa-Garcia, Electroanalysis 10 (1998) 701–706.
- [8] A. Daniel, A.R. Baker, C.M.G. van den Berg, Fresenius J. Anal. Chem. 358 (1997) 703–710.
- [9] J.F. van Staden, M.C. Matoetoe, Anal. Chim. Acta 411 (2000) 201–207.
- [10] M.R. Gongora-Rubio, M.B.A. Fontes, Z.M. da Rocha, E.M. Richter, L. Angnes, Sens. Actuators B 103 (2004) 468–473.
- [11] W. Martinotti, G. Queirazza, A. Guarinoni, G. Mori, Anal. Chim. Acta 305 (1995) 183–191.
- [12] S. Suteerapatarnon, J. Jakmunee, Y. Vaneesorn, K. Grudpan, Talanta 58 (2002) 1235–1242.
- [13] E. Munoz, S. Palmero, Food Chem. 94 (2006) 478–483.
- [14] J. Wang, B.M. Tian, J.Y. Wang, Anal. Commun. 35 (1998) 241–243.
- [15] K.C. Armstrong, C.E. Tatum, R.N. Dansby-Sparks, J.Q. Chambers, Z.-L. Xue, Talanta 82 (2010) 675–680.
- [16] A. Economou, A. Voulgaropoulos, Talanta 71 (2007) 758–765.
- [17] M.Á.G. Ricoa, M. Olivares-Marínb, E.P. Gil, Talanta 80 (2009) 631–635.
- [18] D. Floner, F. Geneste, Electrochem. Commun. 9 (2007) 2271–2275.
- [19] G. Chamoulaud, D. Floner, C. Moinet, C. Lamy, E.M. Belgsir, Electrochim. Acta 46 (2001) 2757–2760.
- [20] T. Romann, E. Lust, Electrochim. Acta 55 (2010) 5746–5752.
- [21] J. Lastincova, L. Jurica, E. Beinrohr, Pol. J. Environ. Stud. 13 (2004) 533–536.
- [22] L. Jurica, A. Manova, J. Dzurov, E. Beinrohr, J.A.C. Broekaert, Fresenius J. Anal. Chem. 366 (2000) 260–266.
- [23] E. Beinrohr, M. Cakrt, J. Dzurov, L. Jurica, J.A.C. Broekaert, Electroanalysis 11 (1999) 1137–1144.
- [24] N.K. Djane, S. Armalis, K. Ndung'u, G. Johansson, L. Mathiasson, Analyst 123 (1998) 393–396.
- [25] D.J. Curran, T.P. Tougas, Anal. Chem. 56 (1984) 672–678.
- [26] W.J. Blaedel, J. Wang, Anal. Chem. 51 (1979) 799–802.
- [27] F. Geneste, C. Moinet, New J. Chem. 28 (2004) 722–726.
- [28] F. Geneste, C. Moinet, S. Ababou-Girard, F. Solal, New J. Chem. 29 (2005) 1520–1526.
- [29] F. Geneste, C. Moinet, J. Electroanal. Chem. 594 (2006) 105–110.
- [30] Y. Kashiwagi, F. Kurashima, S. Chiba, J.-I. Anzai, T. Osa, J.M. Bobbitt, Chem. Commun. (2003) 114–115.
- [31] P. Jego-Evanno, J.P. Hurvois, C. Moinet, J. Electroanal. Chem. 507 (2001) 270–274.
- [32] R. Nasraoui, J.F. Bergamini, S. Ababou-Girard, F. Geneste, J. Solid State Electrochem. 15 (2011) 139–146.
- [33] R. Nasraoui, D. Floner, C. Paul-Roth, F. Geneste, J. Electroanal. Chem. 638 (2010) 9–14.
- [34] R. Nasraoui, D. Floner, F. Geneste, Electrochem. Commun. 12 (2010) 98–100.
- [35] A.L. Tomat, M.L. Costa, C.T. Arranz, Nutrition 27 (2011) 392–398.
- [36] W. Maret, H.H. Sandstead, J. Trace Elem. Med. Biol. 20 (2006) 3–18.
- [37] C. Moinet, J. Phys. IV 4 (1994) C1–175.
- [38] N. Serrano, A. Alberich, J. Manuel, J.M. Diaz-Cruz, C. Arino, M. Esteban, Electrochim. Acta 53 (2008) 6616–6622.
- [39] A. Krolicka, A. Bobrowski, A. Kowal, Electroanalysis 18 (2006) 1649–1657.
- [40] T.-H. Lu, H.-Y. Yang, I.W. Sun, Talanta 49 (1999) 59–68.
- [41] C.M.A. Brett, J.L.F.C. Lima, M.B. Quinaz Garcia, Analyst 119 (1994) 1229–1233.
- [42] C.M.A. Brett, M.B. Quinaz Garcia, J.L.F.C. Lima, Electroanalysis 8 (1996) 1169–1173.